

On the Duality of Global Finite Element Discretization Error-Control in Small Strain Newtonian and Eshelbian Mechanics

M. Rüter, E. Stein

Dedicated to the memory of Dipl.–Ing. Jürgen Olschewski.[†]

In this paper global a posteriori error estimators are presented for the error obtained during the finite element discretization of the linear elasticity problem. Thereby, the duality of global error measures is established that are chosen within the framework of traditional Newtonian mechanics as well as within the framework of Eshelbian mechanics. In Newtonian mechanics we are concerned with the (physical) Cauchy stress tensor that reflects the internal resistance of an elastic body to an applied physical force, whereas in Eshelbian mechanics the applied force is a material force acting on a defect of the elastic body with associated (material) (Newton-)Eshelby stress tensor which is the dual stress tensor of the Cauchy stress tensor. The derivation of a posteriori error estimators is based on the well-established strategy of solving an auxiliary dual problem in order to control the global error measures defined in terms of bounded non-linear functionals. In this paper, two principally different strategies are presented to estimate the error measure. The first strategy rests upon an equilibrated residual error estimator based on local Neumann problems, whereas the second one makes use of averaging techniques. The paper is concluded by a numerical example that illustrates our theoretical results.

1 Introduction

Whenever defects of a material are considered, such as cracks in fracture mechanics, the appropriate framework is the one of Eshelbian mechanics, cf. Eshelby (1951), Maugin (1993), Kienzler and Herrmann (2000), Steinmann (2000) and others, rather than Newtonian mechanics. In Eshelbian mechanics, the material force acting on a defect describes the change in the total potential energy of the elastic body. Hence, if the material is defect free, no material forces are acting on the elastic body. However, if we consider the material forces as obtained by a finite element discretization of the associated model problem within Newtonian mechanics, the material forces are not vanishing because of the finite element discretization error. Different attempts have been made to minimize these discrete material forces which should, at best, vanish. Most attempts use r -adaptive methods based on optimization strategies where only the nodes of the finite element mesh are moved, see e.g. Mueller and Maugin (2002) and Kuhl et al. (2003). To our knowledge, h -, p - or hp -adaptive methods – based on a posteriori error-control – have not been used so far.

The derivation of a posteriori error estimators within the framework of Eshelbian mechanics requires a special approach widely known as goal-oriented error estimation. This technique generalizes the canonical approach in estimating the error in the (global) energy norm to more general error measures given by (linear or linearized) functionals, whereby we restrict our considerations in this paper to global error measures in Newtonian as well as in Eshelbian mechanics. As introduced in the seminal work by Eriksson et al. (1995) and developed further by Becker and Rannacher (1996) and others, goal-oriented a posteriori error estimators are based on the widely used strategy of solving an auxiliary dual problem. Thus, a key feature in this context is the construction of the dual data. The presented a posteriori error estimators are based either on the residuals of both the original and the dual problem or on recovery of the associated stress fields. For the residual type error estimators we make the choice of implicit error estimators of equilibrated residual type based on local Neumann problems, whereby one of the proposed estimators was originally introduced by Prudhomme and Oden (1999) and Ohnibus et al. (2001) for the linear elasticity problem.

[†]The late Jürgen Olschewski worked at our institute from 1978 to 1981 on the research project “Theoretical and numerical investigation of thermo-mechanical deformations of mineral salt including damage”. He was a brilliant scientist in the fields of thermodynamics of solids and of material theory and brought new ideas for constitutive equations as well as suitable engineering solutions matching with test results. We are very sorry that we couldn’t convince him to become a Dr.–Ing. in appreciation of his excellent research results.

The paper is outlined as follows: In Section 2 the boundary value problem of linear elasticity is briefly introduced within the framework of Newtonian and Eshelbian mechanics. In the following section, global error measures in Newtonian and Eshelbian mechanics are established. Furthermore, error representations are derived that are based on the solution of an auxiliary dual problem, and the construction of the dual data is discussed. Subsequently, in Section 4 a posteriori error estimators of equilibrated residual type based on local Neumann problems and, additionally, error estimators using averaging techniques are derived. Finally, in Section 5 an illustrative numerical example is presented.

2 The Model Problem

In this section we first introduce the model problem of linear elasticity in the framework of traditional Newtonian mechanics. Furthermore, we establish the associated Eshelbian formulation. In both frameworks the elastic body occupies the closure of a bounded open set $\Omega \subset \mathbb{R}^3$ with piecewise smooth and Lipschitz continuous boundary Γ such that $\Gamma = \bar{\Gamma}_D \cup \bar{\Gamma}_N$ and $\Gamma_D \cap \Gamma_N = \emptyset$, where Γ_D and Γ_N are the Dirichlet and Neumann boundaries, respectively. For the sake of simplicity, the elastic body is assumed to be isotropic and homogeneous.

2.1 Newtonian Mechanics

To begin with, let us consider the model problem as described within traditional Newtonian mechanics. In the strong formulation we seek the displacement field $\mathbf{u} \in [C^2(\Omega)]^3 \cap [C^1(\bar{\Omega})]^3$, such that the field equation

$$\operatorname{div} \boldsymbol{\sigma} = \mathbf{0} \quad \text{in } \Omega \quad (1)$$

and the boundary conditions

$$\mathbf{u} = \mathbf{0} \quad \text{on } \Gamma_D \quad (2a)$$

$$\boldsymbol{\sigma} \cdot \mathbf{n} = \bar{\mathbf{t}}_{phy} \quad \text{on } \Gamma_N \quad (2b)$$

are fulfilled. In the above, $\boldsymbol{\sigma} = \mathbb{C} : \boldsymbol{\varepsilon}$ denotes the symmetric (physical) Cauchy stress tensor, where $\mathbb{C} = \lambda \mathbf{1} \otimes \mathbf{1} + 2\mu \mathbb{I}$ is the constant positive definite fourth-order elasticity tensor with positive Lamé constants λ and μ as well as second-order and fourth-order identity tensors $\mathbf{1}$ and \mathbb{I} , respectively. Furthermore, $\boldsymbol{\varepsilon} = (\operatorname{grad} \mathbf{u})^{sym}$ denotes the strain tensor, \mathbf{n} is the unit outward normal, and $\bar{\mathbf{t}}_{phy} \in [L_2(\Gamma_N)]^3$ are prescribed (physical) tractions on the Neumann boundary Γ_N . Note that body forces are omitted in this formulation.

In the corresponding weak formulation we search for the displacement field \mathbf{u} in the Hilbert space $\mathcal{V} = \{\mathbf{v} \in [H^1(\Omega)]^3 ; \mathbf{v}|_{\Gamma_D} = \mathbf{0}\}$ such that the variational equation

$$a(\mathbf{u}, \mathbf{v}) = F_{phy}(\mathbf{v}) \quad \forall \mathbf{v} \in \mathcal{V} \quad (3)$$

is fulfilled. Here, the bilinear form $a : \mathcal{V} \times \mathcal{V} \rightarrow \mathbb{R}$ and the linear form $F_{phy} : \mathcal{V} \rightarrow \mathbb{R}$ are defined by

$$a(\mathbf{u}, \mathbf{v}) = \int_{\Omega} \boldsymbol{\sigma}(\mathbf{u}) : \boldsymbol{\varepsilon}(\mathbf{v}) \, dV \quad (4)$$

and

$$F_{phy}(\mathbf{v}) = \int_{\Gamma_N} \bar{\mathbf{t}}_{phy} \cdot \mathbf{v} \, dS, \quad (5)$$

respectively. Note that the functional F_{phy} represents physical forces acting on the Neumann boundary Γ_N . Moreover, it should be pointed out that for the chosen model problem a unique solution to the variational problem (3) exists due to the Lax-Milgram theorem. Observe, however, that although the Lax-Milgram theorem ensures the existence of a unique solution $\mathbf{u} \in \mathcal{V}$, Equation (3) is not the unique variational formulation that is satisfied by $\mathbf{u} \in \mathcal{V}$, as we shall see later.

In the associated finite element discretization of the variational problem (3), we subdivide the elastic body into a finite number n_e of connected elements $\bar{\Omega}_e$ such that $\bar{\Omega} \approx \bigcup_{n_e} \bar{\Omega}_e$. On these elements we define polynomials to construct a finite dimensional subspace $\mathcal{V}_h \subset \mathcal{V}$. Thus, in the discrete variational problem we solve

$$a(\mathbf{u}_h, \mathbf{v}_h) = F_{phy}(\mathbf{v}_h) \quad \forall \mathbf{v}_h \in \mathcal{V}_h \quad (6)$$

for the finite element solution $\mathbf{u}_h \in \mathcal{V}_h$. Obviously, a unique solution $\mathbf{u}_h \in \mathcal{V}_h$ to this problem exists, since $\mathcal{V}_h \subset \mathcal{V}$.

2.2 Eshelbian Mechanics

Within the framework of Eshelbian mechanics, analogously to (1) and (2) the strong solution $\mathbf{u} \in [C^2(\Omega)]^3 \cap [C^1(\bar{\Omega})]^3$ to the boundary value problem defined by (1) and (2) satisfies the field equation

$$\operatorname{div} \Sigma = \mathbf{0} \quad \text{in } \Omega \quad (7)$$

in case of a homogeneous elastic body. Here, $\Sigma = W_s \mathbf{1} - (\operatorname{grad} \mathbf{u})^T \cdot \boldsymbol{\sigma}$ denotes the non-symmetric and non-linear (material) Newton-Eshelby stress tensor with specific strain-energy function $W_s = \frac{1}{2} \boldsymbol{\sigma} : \boldsymbol{\varepsilon}$. The boundary conditions, however, cannot be chosen arbitrarily, since they are a direct consequence of the ones within the framework of Newtonian mechanics. More precisely, we have

$$\mathbf{u} = \mathbf{0} \quad \text{on } \Gamma_D \quad (8a)$$

$$\bar{\Sigma} \cdot \mathbf{n} = \mathbf{t}_{mat} \quad \text{on } \Gamma_N, \quad (8b)$$

where $\mathbf{t}_{mat} \in [L_2(\Gamma_N)]^3$ denotes the (material) traction vector. Note carefully that within Eshelbian mechanics the material tractions \mathbf{t}_{mat} are not prescribed, since in this case the Newton-Eshelby stress tensor is prescribed (denoted by the bar). Thus, (8b) is not a boundary condition in the sense that (7) and (8) do not represent a boundary value problem.

As a consequence, the weak solution $\mathbf{u} \in \mathcal{V}$ to the linear variational problem (3) also satisfies the non-linear weak formulation of (7) and (8), i.e.

$$b(\mathbf{u}, \mathbf{v}) = F_{mat}(\mathbf{v}) \quad \forall \mathbf{v} \in \mathcal{V}. \quad (9)$$

Note, however, that this variational equation does not represent the weak form of a boundary value problem. In the above, the semi-linear form $b : \mathcal{V} \times \mathcal{V} \rightarrow \mathbb{R}$, i.e. b is linear with respect to its second argument only, and the linear form $F_{mat} : \mathcal{V} \rightarrow \mathbb{R}$ are defined by

$$b(\mathbf{u}, \mathbf{v}) = \int_{\Omega} \Sigma(\mathbf{u}) : \operatorname{grad} \mathbf{v} \, dV \quad (10)$$

and

$$F_{mat}(\mathbf{v}) = \int_{\Gamma_N} \mathbf{t}_{mat} \cdot \mathbf{v} \, dS, \quad (11)$$

respectively. We remark that the functional F_{mat} represents material forces acting on Γ_N .

It should be stressed that although $\mathbf{u} \in \mathcal{V}$ fulfills both the variational equations (3) and (9), because of the finite element discretization error

$$\mathbf{e}_u = \mathbf{u} - \mathbf{u}_h \quad (12)$$

the solution $\mathbf{u}_h \in \mathcal{V}_h$ of the discretized variational problem (6) does not in general satisfy the finite element discretization of (9), i.e.

$$b(\mathbf{u}_h, \mathbf{v}_h) \neq F_{mat}(\mathbf{v}_h) \quad \forall \mathbf{v}_h \in \mathcal{V}_h. \quad (13)$$

This fundamentally important fact has, as we shall see later, consequences concerning the error analysis.

3 The Finite Element Discretization Error

In what follows we establish error representation formulas in a Newtonian as well as in an Eshelbian setting that serve as a basis for the subsequent a posteriori error analysis.

3.1 Nodal Physical and Material Forces

Upon inserting the finite element approximation $\mathbf{u}_h \in \mathcal{V}_h$ into the variational equation (3), we obtain a non-vanishing linear functional $R_{phy,u} : \mathcal{V} \rightarrow \mathbb{R}$ (in case that $\mathbf{e}_u \neq \mathbf{0}$) defined by

$$R_{phy,u}(\mathbf{v}) = F_{phy}(\mathbf{v}) - a(\mathbf{u}_h, \mathbf{v}) \quad (14)$$

which is also referred to as the (physical) weak form of the residual. Recalling the finite element discretization (6), it is a simple observation that the weak form of the residual (14) vanishes for all functions $\mathbf{v}_h \in \mathcal{V}_h$, i.e. $R_{phy,u}(\mathbf{v}_h) = 0$, since $\mathbf{u}_h \in \mathcal{V}_h$ is the exact solution of (6). This important property is called the Galerkin orthogonality. With the definition of the linear form (5) and the bilinear form (4) at hand, the Galerkin orthogonality can be expressed by

$$R_{phy,u}(\mathbf{v}_h) = \sum_{n_e} \hat{\mathbf{v}}^T \{ \mathbf{F}_{phy,e}^{ext} - \mathbf{F}_{phy,e}^{int} \} = 0 \quad (15)$$

with energy-equivalent exterior nodal physical forces

$$\mathbf{F}_{phy,e}^{ext} = \int_{\partial\Omega_e} \mathbf{N}^T \mathbf{t}_{phy}(\mathbf{u}_h|_{\bar{\Omega}_e}) \, dS \quad (16)$$

and energy-equivalent interior nodal physical forces

$$\mathbf{F}_{phy,e}^{int} = \int_{\Omega_e} \mathbf{B}^T \boldsymbol{\sigma}(\mathbf{u}_h|_{\bar{\Omega}_e}) \, dV. \quad (17)$$

In the above, $\hat{\mathbf{v}}$ are nodal values of the test functions \mathbf{v}_h associated to the nodes $\mathbf{X}_k \in \bar{\Omega}_e$, \mathbf{N} is the usual matrix of the finite element ansatz functions N , and \mathbf{B} denotes the so-called \mathbf{B} -matrix consisting of the derivatives of the ansatz functions N according to the definition of strains. Since the test functions $\mathbf{v}_h|_{\bar{\Omega}_e} = \mathbf{N}\hat{\mathbf{v}}$ can be chosen arbitrarily, at each element Ω_e the interior and exterior nodal physical forces are in equilibrium, i.e.

$$\mathbf{F}_{phy,e}^{int} = \mathbf{F}_{phy,e}^{ext}. \quad (18)$$

Consequently, upon summing up the interior or exterior nodal physical forces associated to one node $\mathbf{X}_k \in \Omega$, that means summing up the contributions from the nodal patch, i.e. from the adjacent elements, the resulting nodal physical forces at each node \mathbf{X}_k vanish.

Likewise, we may insert \mathbf{u}_h into the variational equation (9) to derive the (material) weak form of the residual $R_{mat,u} : \mathcal{V} \rightarrow \mathbb{R}$ within the framework of Eshelbian mechanics that is defined by

$$R_{mat,u}(\mathbf{v}) = F_{mat}(\mathbf{v}) - b(\mathbf{u}_h, \mathbf{v}). \quad (19)$$

However, as mentioned before, $\mathbf{u}_h \in \mathcal{V}_h$ does generally not satisfy the finite element discretization of (9), cf. (13). As a consequence, the weak form of the residual (19) does generally not vanish for arbitrary test functions $\mathbf{v}_h \in \mathcal{V}_h$, i.e. $R_{mat,u}(\mathbf{v}_h) \neq 0$. Hence, the Galerkin orthogonality does not hold within the framework of Eshelbian mechanics which can – similarly to (15) – be expressed as

$$R_{mat,u}(\mathbf{v}_h) = \sum_{n_e} \hat{\mathbf{v}}^T \{ \mathbf{F}_{mat,e}^{ext} - \mathbf{F}_{mat,e}^{int} \} \neq 0 \quad (20)$$

with energy-equivalent exterior nodal material forces

$$\mathbf{F}_{mat,e}^{ext} = \int_{\partial\Omega_e} \mathbf{N}^T \mathbf{t}_{mat}(\mathbf{u}_h|_{\bar{\Omega}_e}) \, dS \quad (21)$$

and energy-equivalent interior nodal material forces

$$\mathbf{F}_{mat,e}^{int} = \int_{\Omega_e} \mathbf{B}^T \boldsymbol{\Sigma}(\mathbf{u}_h|_{\bar{\Omega}_e}) \, dV. \quad (22)$$

Apparently, since the (material) weak form of the residual (20) does not vanish or, in other words, since $\mathbf{u}_h \in \mathcal{V}_h$ is not the exact solution of (13), the exterior and interior material forces are not in equilibrium, i.e.

$$\mathbf{F}_{mat,e}^{int} \neq \mathbf{F}_{mat,e}^{ext}. \quad (23)$$

Thus, it should be noted that upon summing up the interior or exterior nodal material forces associated to one node $\mathbf{X}_k \in \Omega$, the nodal material forces at each node \mathbf{X}_k do not vanish. Since this is a direct consequence of the residual (20), we refer to these non-vanishing material forces as *residual material forces* rather than “spurious material forces” as suggested by other authors, see e.g. Steinmann et al. (2001). The residual material forces vanish only, if $R_{mat,u}(\mathbf{v}_h) = 0$ for all $\mathbf{v}_h \in \mathcal{V}_h$, i.e. either if we found the exact solution $\mathbf{u} \in \mathcal{V}$ to (3) which also satisfies (9) or if we found a discrete solution that satisfies the finite element discretization of (9). Consequently, if we aim at modifying the finite element solution \mathbf{u}_h of (6) (by moving the nodes or, in other words, by changing the finite element test and solution space \mathcal{V}_h) in such a fashion that, at best, the residual material forces vanish, nothing can be said about the finite element discretization error \mathbf{e}_u . Thus, from the viewpoint of error-controlled adaptive finite element methods, it is not useful to put efforts in finding such a modified discrete solution, since although residual material forces are an indicator for the discretization error, the converse is obviously not true, i.e. vanishing residual material forces are not an indicator for a vanishing discretization error.

3.2 Error Representation Formulas for the Finite Element Discretization Error

Our objective in this paper is to control the discretization error \mathbf{e}_u in terms of adaptive finite element methods based on a posteriori error estimates. In order to derive such a posteriori error estimates, we shall first establish the exact error representation formulas which serve as a starting point to derive error estimators. An exact error representation formula in the framework of Newtonian mechanics is simply derived by recalling the definition of the weak form of the residual (14) and making use of the variational equation (3) and the linearity properties of the bilinear form a . Hence, we get

$$a(\mathbf{e}_u, \mathbf{v}) = R_{phy,u}(\mathbf{v}) \quad \forall \mathbf{v} \in \mathcal{V} \quad (24)$$

which is a variational equation for the unknown error $\mathbf{e}_u \in \mathcal{V}$.

In the same manner we can derive an error representation formula for the error \mathbf{e}_u within Eshelbian mechanics. Hence, we first replace the linear functional F_{mat} in (19) with the semi-linear form b according to the variational equation (9) to see that $R_{mat,u}$ takes the form

$$R_{mat,u}(\mathbf{v}) = b(\mathbf{u}, \mathbf{v}) - b(\mathbf{u}_h, \mathbf{v}). \quad (25)$$

Since b is semi-linear, we next apply the fundamental theorem of calculus (cf. Eriksson et al. (1995), Becker and Rannacher (1996)) on b which yields

$$b(\mathbf{u}, \mathbf{v}) - b(\mathbf{u}_h, \mathbf{v}) = \int_0^1 b'(\boldsymbol{\xi}(s); \mathbf{e}_u, \mathbf{v}) \, ds \quad (26)$$

with $\boldsymbol{\xi}(s) = \mathbf{u}_h + s \mathbf{e}_u$, whereby $s \in [0, 1]$, and the bilinear form $b' : \mathcal{V} \times \mathcal{V} \rightarrow \mathbb{R}$ being the tangent form of b defined as

$$b'(\boldsymbol{\xi}(s); \mathbf{e}_u, \mathbf{v}) = D_{\mathbf{u}} b(\mathbf{u}, \mathbf{v})|_{\boldsymbol{\xi}(s)} \cdot \mathbf{e}_u \quad (27a)$$

$$= \int_{\Omega} [\boldsymbol{\varepsilon}(\boldsymbol{\xi}(s)) : \boldsymbol{\sigma}(\mathbf{e}_u)] \operatorname{div} \mathbf{v} - [(\operatorname{grad} \mathbf{e}_u)^T \cdot \boldsymbol{\sigma}(\boldsymbol{\xi}(s)) + (\operatorname{grad} \boldsymbol{\xi}(s))^T \cdot \boldsymbol{\sigma}(\mathbf{e}_u)] : \operatorname{grad} \mathbf{v} \, dV, \quad (27b)$$

i.e. the Gâteaux-derivative of b with respect to \mathbf{u} . Since b' is bilinear, we may next introduce the secant form of b , that is the bilinear form $b_S : \mathcal{V} \times \mathcal{V} \rightarrow \mathbb{R}$ defined as

$$b_S(\mathbf{u}, \mathbf{u}_h; \mathbf{e}_u, \mathbf{v}) = \int_0^1 b'(\boldsymbol{\xi}(s); \mathbf{e}_u, \mathbf{v}) \, ds. \quad (28)$$

Upon summing up (25), (26) and (28), we thus arrive at the exact error representation formula in an Eshelbian setting

$$b_S(\mathbf{u}, \mathbf{u}_h; \mathbf{e}_u, \mathbf{v}) = R_{mat,u}(\mathbf{v}) \quad \forall \mathbf{v} \in \mathcal{V} \quad (29)$$

which has a similar structure to (24) but also depends on the exact solution $\mathbf{u} \in \mathcal{V}$ and on the finite element solution $\mathbf{u}_h \in \mathcal{V}_h$.

3.3 Global Error Measures

It should be clear, however, that the error representation formulas (24) and (29) are generally not solvable, since the variational problems are infinite dimensional. Furthermore, in case of (24), the finite element discretization error \mathbf{e}_u cannot be approximated in \mathcal{V}_h , since the weak form of the residual vanishes in this case due to the Galerkin orthogonality as we have seen above. Apart from that, the knowledge of an estimation of the error \mathbf{e}_u itself is of less use in order to drive an adaptive mesh refinement scheme, since a mapping of the error onto the set of real numbers is required. Therefore, it proves useful to introduce an arbitrary global goal-quantity of interest $Q : \mathcal{V} \rightarrow \mathbb{R}$ that can be any linear or non-linear bounded functional that is defined over the entire domain Ω . We remark that Q can also be defined as a local goal-quantity of interest. Within the framework of Newtonian mechanics, such a local goal-quantity of interest can be mean displacements on a portion of the Neumann boundary Γ_N or mean stress distributions in a subdomain of the elastic body Ω , whereas a typical example in Eshelbian mechanics is the J -integral as a fracture criterion, see e.g. Rüter and Stein (2002), Heintz et al. (2002) and Stein et al. (2004). In

this contribution, however, we shall confine ourselves to the case of global functionals Q . Since Q is non-linear in general, we may define the associated general error measure $E : \mathcal{V} \times \mathcal{V} \rightarrow \mathbb{R}$ either as the error of the quantity, i.e. $E(\mathbf{u}, \mathbf{u}_h) = Q(\mathbf{u}) - Q(\mathbf{u}_h)$, or as the quantity of the error $E(\mathbf{u}, \mathbf{u}_h) = Q(\mathbf{e}_u)$, where we adopted the notation as introduced by Larsson et al. (2002).

Upon recalling the error representation formula (24) within the framework of Newtonian mechanics, a natural choice for an appropriate goal-quantity of interest Q is the non-linear energy functional

$$Q(\mathbf{u}) = a(\mathbf{u}, \mathbf{u}) = \int_{\Omega} \boldsymbol{\sigma}(\mathbf{u}) : \boldsymbol{\varepsilon}(\mathbf{u}) \, dV. \quad (30)$$

Note carefully that although this functional is non-linear (more precisely: quadratic), we observe the important property that $Q(\mathbf{u}) - Q(\mathbf{u}_h) = Q(\mathbf{e}_u)$ due to the Galerkin orthogonality. Hence, the error measure E yields the same value in either case $E(\mathbf{u}, \mathbf{u}_h) = Q(\mathbf{u}) - Q(\mathbf{u}_h)$ and $E(\mathbf{u}, \mathbf{u}_h) = Q(\mathbf{e}_u)$ which is none other than the well-known statement that the error of the energy is equal to the energy of the error. In practical error estimation techniques it turns out, however, that the energy norm of the error, i.e. $\|\mathbf{e}_u\| = a(\mathbf{e}_u, \mathbf{e}_u)^{\frac{1}{2}}$, is the appropriate error measure.

Likewise, in the case of Eshelbian mechanics the natural error measure with respect to the error representation formula (29) were $b_S(\mathbf{u}, \mathbf{u}_h; \mathbf{e}_u, \mathbf{e}_u)$. It should be stressed, however, that this error measure depends on the (unknown) exact solution \mathbf{u} and on the (mesh dependent) finite element solution $\mathbf{u}_h \in \mathcal{V}_h$. Therefore, similarly to (30), we define the goal-quantity of interest Q as the non-linear functional

$$Q(\mathbf{u}) = b(\mathbf{u}, \mathbf{u}) = \int_{\Omega} \boldsymbol{\Sigma}(\mathbf{u}) : \text{grad } \mathbf{u} \, dV. \quad (31)$$

Then, the appropriate error measure is defined as $E(\mathbf{u}, \mathbf{u}_h) = Q(\mathbf{u}) - Q(\mathbf{u}_h)$. Note that in this case we observe that $Q(\mathbf{u}) - Q(\mathbf{u}_h) \neq Q(\mathbf{e}_u)$.

Since the above defined error measures E are non-linear in either case, we apply essentially the same steps as in Section 3.2, i.e. we first employ the fundamental theorem of calculus on

$$E(\mathbf{u}, \mathbf{u}_h) = E(\mathbf{u}, \mathbf{u}_h) - E(\mathbf{u}_h, \mathbf{u}_h), \quad (32)$$

whereby it should be noted that clearly $E(\mathbf{u}_h, \mathbf{u}_h) = 0$, which yields

$$E(\mathbf{u}, \mathbf{u}) - E(\mathbf{u}, \mathbf{u}_h) = \int_0^1 E'(\boldsymbol{\xi}(s); \mathbf{e}_u) \, ds \quad (33)$$

with tangent form

$$E'(\boldsymbol{\xi}(s); \mathbf{e}_u) = D_{\mathbf{u}} E(\mathbf{u}, \mathbf{u}_h)|_{\boldsymbol{\xi}(s)} \cdot \mathbf{e}_u. \quad (34)$$

Since the tangent form E' is a linear functional, we next introduce the secant form

$$E_S(\mathbf{u}, \mathbf{u}_h; \mathbf{e}_u) = \int_0^1 E'(\boldsymbol{\xi}(s); \mathbf{e}_u) \, ds \quad (35)$$

to see that the error measure E can be represented as

$$E(\mathbf{u}, \mathbf{u}_h) = E_S(\mathbf{u}, \mathbf{u}_h; \mathbf{e}_u). \quad (36)$$

Since E_S involves the exact solution $\mathbf{u} \in \mathcal{V}$, we shall next introduce an approximation E_T of E_S by replacing the exact solution $\mathbf{u} \in \mathcal{V}$ with the finite element solution $\mathbf{u}_h \in \mathcal{V}_h$. We thus arrive at the tangent form

$$E_T(\cdot) = E_S(\mathbf{u}_h, \mathbf{u}_h; \cdot) \quad (37a)$$

$$\approx E_S(\mathbf{u}, \mathbf{u}_h; \cdot), \quad (37b)$$

which holds for small errors \mathbf{e}_u only. More precisely, in the case where the goal-quantity of interest Q is defined as in (30), the tangent form takes the form

$$E_T(\mathbf{e}_u) = 2a(\mathbf{u}_h, \mathbf{e}_u) \quad (38)$$

and vanishes due to the Galerkin orthogonality. In case of (31), however, we obtain the non-vanishing functional

$$E_T(\mathbf{e}_u) = b'(\mathbf{u}_h; \mathbf{e}_u, \mathbf{u}_h) + b(\mathbf{u}_h, \mathbf{e}_u) \quad (39a)$$

$$\begin{aligned} &= \int_{\Omega} [\boldsymbol{\varepsilon}(\mathbf{u}_h) : \boldsymbol{\sigma}(\mathbf{e}_u)] \text{div } \mathbf{u}_h - [(\text{grad } \mathbf{e}_u)^T \cdot \boldsymbol{\sigma}(\mathbf{u}_h) + (\text{grad } \mathbf{u}_h)^T \cdot \boldsymbol{\sigma}(\mathbf{e}_u)] : \text{grad } \mathbf{u}_h \, dV \\ &+ \int_{\Omega} \boldsymbol{\Sigma}(\mathbf{u}_h) : \text{grad } \mathbf{e}_u \, dV. \end{aligned} \quad (39b)$$

3.4 Error Representation Formulas for the Global Error Measure E

In order to derive an error representation formula for the error measure E , we follow the well-established strategy of solving an auxiliary dual variational problem which reads: find a solution $\mathbf{g} \in \mathcal{V}$ satisfying

$$a^*(\mathbf{g}, \mathbf{v}) = E_S(\mathbf{u}, \mathbf{u}_h; \mathbf{v}) \quad \forall \mathbf{v} \in \mathcal{V}. \quad (40)$$

Here, $a^* : \mathcal{V} \times \mathcal{V} \rightarrow \mathbb{R}$ denotes the dual bilinear form of a that coincides with a in case of the linear elasticity problem because of the symmetry of a . An exact error representation formula in terms of the solution of the dual problem is now simply obtained by setting $\mathbf{v} = \mathbf{e}_u$ in (40) and reads with (36)

$$E(\mathbf{u}, \mathbf{u}_h) = E_S(\mathbf{u}, \mathbf{u}_h; \mathbf{e}_u) = a^*(\mathbf{g} - \pi\mathbf{g}, \mathbf{e}_u) \quad (41)$$

for any $\pi\mathbf{g} \in \mathcal{V}_h$ due to the Galerkin orthogonality. Thus, a practically useful error representation formula can only be obtained within the framework of Newtonian mechanics, although clearly the error measure E may either be defined in Newtonian or in Eshelbian mechanics. Note also that in the case where the functional Q is defined as in (30) we clearly obtain $\mathbf{g} = \mathbf{u}$, i.e. the dual problem coincides with the primal problem. We further remark that although $\pi\mathbf{g}$ can be chosen arbitrarily, it proves convenient in the a posteriori error analysis to define $\pi\mathbf{g}$ either as some projection of the dual solution \mathbf{g} or as the finite element solution $\mathbf{g}_h \in \mathcal{V}_h$ of the discrete dual problem

$$a^*(\mathbf{g}_h, \mathbf{v}_h) = E_S(\mathbf{u}, \mathbf{u}_h; \mathbf{v}_h) \quad \forall \mathbf{v}_h \in \mathcal{V}_h \quad (42)$$

as the best approximation of \mathbf{g} in \mathcal{V}_h . Doing this, we may further introduce the finite element discretization error $\mathbf{e}_g = \mathbf{g} - \mathbf{g}_h$ of the dual problem and, consequently, the associated exact error representation

$$a^*(\mathbf{e}_g, \mathbf{v}) = R_{phy,g}(\mathbf{v}) \quad \forall \mathbf{v} \in \mathcal{V}, \quad (43)$$

where the (physical) weak form of the residual of the dual problem $R_{phy,g} : \mathcal{V} \rightarrow \mathbb{R}$ is similarly to $R_{phy,u}$ defined as

$$R_{phy,g}(\mathbf{v}) = E_S(\mathbf{u}, \mathbf{u}_h; \mathbf{v}) - a^*(\mathbf{g}_h, \mathbf{v}). \quad (44)$$

It has already been pointed out that the main difficulty with error representation formulas such as (41) and (43) arises from the unknown exact solution $\mathbf{u} \in \mathcal{V}$ that appears in the secant form E_S . As we saw earlier, for small errors \mathbf{e}_u it is sufficient to use the approximation E_T . Thus, we obtain the approximate dual variational problem

$$a^*(\mathbf{g}, \mathbf{v}) = E_T(\mathbf{v}) \quad \forall \mathbf{v} \in \mathcal{V} \quad (45)$$

leading to the approximate error representation

$$E(\mathbf{u}, \mathbf{u}_h) = E_T(\mathbf{e}_u) = a^*(\mathbf{g} - \pi\mathbf{g}, \mathbf{e}_u) \quad (46)$$

for any $\pi\mathbf{g} \in \mathcal{V}_h$ which is restricted to small errors \mathbf{e}_u . In particular, if we choose $\pi\mathbf{g}$ to be the finite element solution \mathbf{g}_h of the discretized (approximate) dual problem (45), i.e.

$$a^*(\mathbf{g}_h, \mathbf{v}_h) = E_T(\mathbf{v}_h) \quad \forall \mathbf{v}_h \in \mathcal{V}_h, \quad (47)$$

we may further approximate the error representation (43) by

$$a^*(\mathbf{e}_g, \mathbf{v}) = \bar{R}_{phy,g}(\mathbf{v}) \quad \forall \mathbf{v} \in \mathcal{V} \quad (48)$$

with approximated (physical) weak form of the residual

$$\bar{R}_{phy,g}(\mathbf{v}) = E_T(\mathbf{v}) - a^*(\mathbf{g}_h, \mathbf{v}). \quad (49)$$

Finally, we may combine the presented exact error representations (24), (41) and (43) to get the result

$$E(\mathbf{u}, \mathbf{u}_h) = R_{phy,u}(\mathbf{g} - \pi\mathbf{g}) = R_{phy,g}(\mathbf{e}_u), \quad (50)$$

which can be interpreted as Betti's theorem, also known as the reciprocity theorem, see also Cirak and Ramm (1998).

4 A Posteriori Error Estimation

With the above considerations in mind, different strategies for the a posteriori estimation of the error measure E can be envisioned.

4.1 The General Strategy

To illustrate the main idea, we begin with the general strategy for self-adjoint operators to obtain upper error bounds that can be sketched as follows

$$|E(\mathbf{u}, \mathbf{u}_h)| = |a(\mathbf{e}_u, \mathbf{e}_g)| \quad (51a)$$

$$\leq \|\mathbf{e}_u\| \|\mathbf{e}_g\|. \quad (51b)$$

Note that equality only holds in case of (30). It is easy to see that, by employing the Cauchy-Schwarz inequality, the estimation of the error measure $|E(\mathbf{u}, \mathbf{u}_h)|$ is converted to estimate the discretization error for both the primal and the dual problem in the energy norm for which various methods, mostly residual based, were developed in the last two decades. For an overview we refer to Verfürth (1999) and Ainsworth and Oden (2000). In particular, if the considered energy norm error estimator provides guaranteed upper error bounds, as verified by e.g. a posteriori error estimators of equilibrated residual type based on local Neumann problems, then $|E(\mathbf{u}, \mathbf{u}_h)|$ is bounded above as well. However, it is quite evident that such a bound might not be very sharp due to the unknown angle between the discretization errors \mathbf{e}_u and \mathbf{e}_g . Furthermore, the estimate (51) does not provide an appropriate error indicator on element level which could be used to drive an adaptive mesh refinement algorithm.

To overcome these difficulties, we may now alter the general estimate (51) by involving decoupled element contributions as follows

$$|E(\mathbf{u}, \mathbf{u}_h)| = \left| \sum_{n_e} a_e(\mathbf{e}_u|_{\bar{\Omega}_e}, \mathbf{e}_g|_{\bar{\Omega}_e}) \right| \quad (52a)$$

$$\leq \sum_{n_e} |a_e(\mathbf{e}_u|_{\bar{\Omega}_e}, \mathbf{e}_g|_{\bar{\Omega}_e})| \quad (52b)$$

$$\leq \sum_{n_e} \|\mathbf{e}_u|_{\bar{\Omega}_e}\|_{\Omega_e} \|\mathbf{e}_g|_{\bar{\Omega}_e}\|_{\Omega_e} \quad (52c)$$

$$\leq \|\mathbf{e}_u\| \|\mathbf{e}_g\|. \quad (52d)$$

Here, $a_e : \mathcal{V}_e \times \mathcal{V}_e \rightarrow \mathbb{R}$, with local test and solution space $\mathcal{V}_e = \{\mathbf{v}|_{\bar{\Omega}_e} : \mathbf{v} \in \mathcal{V}\}$ and associated local norm $\|\cdot\|_{\Omega_e} = a_e(\cdot, \cdot)^{\frac{1}{2}}$, denotes the restriction of the bilinear form a to an element $\bar{\Omega}_e$ such that

$$a(\mathbf{u}, \mathbf{v}) = \sum_{n_e} a_e(\mathbf{u}|_{\bar{\Omega}_e}, \mathbf{v}|_{\bar{\Omega}_e}) \quad \forall \mathbf{u}, \mathbf{v} \in \mathcal{V}. \quad (53)$$

Next, let us assume that we can compute approximations $\varphi_e \in \mathcal{V}_e$ and $\chi_e \in \mathcal{V}_e$ of the local error contributions $\mathbf{e}_u|_{\bar{\Omega}_e} \in \mathcal{V}_e$ and $\mathbf{e}_g|_{\bar{\Omega}_e} \in \mathcal{V}_e$ such that

$$\mathbf{e}_u|_{\bar{\Omega}_e} = \varphi_e + \hat{\varphi}_e \quad \text{and} \quad \mathbf{e}_g|_{\bar{\Omega}_e} = \chi_e + \hat{\chi}_e \quad (54)$$

hold with “small” $\hat{\varphi}_e, \hat{\chi}_e \in \mathcal{V}_e$. Upon inserting the approximations (54) in the estimates (52a) or (52b), let us further assume that the approximations φ_e and χ_e are suitable in the sense that

$$a_e(\mathbf{e}_u|_{\bar{\Omega}_e}, \mathbf{e}_g|_{\bar{\Omega}_e}) \approx a_e(\varphi_e, \chi_e). \quad (55)$$

In other words, the contributions containing either $\hat{\varphi}_e$ or $\hat{\chi}_e$ are small of higher order and therefore negligible, cf. Babuška and Strouboulis (2001). If this is the case, we may obviously further introduce the approximations

$$\|\mathbf{e}_u|_{\bar{\Omega}_e}\|_{\Omega_e} \approx \|\varphi_e\|_{\Omega_e} \quad \text{and} \quad \|\mathbf{e}_g|_{\bar{\Omega}_e}\|_{\Omega_e} \approx \|\chi_e\|_{\Omega_e}. \quad (56)$$

With these notations at hand, we may now introduce three abstract a posteriori error estimators in addition to the estimate (51). The first error estimator is based on the estimate (52a) and reads with (55)

$$E(\mathbf{u}, \mathbf{u}_h) \approx \sum_{n_e} a_e(\varphi_e, \chi_e). \quad (57)$$

Note that a possibly sharp error estimator can be obtained in this fashion with the obvious side-effect that the presented estimator has no bounding properties. Therefore, in the second error estimator, we insert (55) in (52b) to get a less sharp error estimator which has, on the other hand, the virtue that it provides an upper error bound as follows

$$E(\mathbf{u}, \mathbf{u}_h) \leq \sum_{n_e} |a_e(\mathbf{e}_u|_{\bar{\Omega}_e}, \mathbf{e}_g|_{\bar{\Omega}_e})| \quad (58a)$$

$$\approx \sum_{n_e} |a_e(\boldsymbol{\varphi}_e, \boldsymbol{\chi}_e)|. \quad (58b)$$

Strictly speaking, however, this upper bound is not guaranteed, since we can approximate the bilinear form $a_e(\mathbf{e}_u|_{\bar{\Omega}_e}, \mathbf{e}_g|_{\bar{\Omega}_e})$ at best. Likewise, we may next insert (56) in (52c) which results in the error estimator

$$|E(\mathbf{u}, \mathbf{u}_h)| \leq \sum_{n_e} \|\mathbf{e}_u|_{\bar{\Omega}_e}\|_{\Omega_e} \|\mathbf{e}_g|_{\bar{\Omega}_e}\|_{\Omega_e} \quad (59a)$$

$$\approx \sum_{n_e} \|\boldsymbol{\varphi}_e\|_{\Omega_e} \|\boldsymbol{\chi}_e\|_{\Omega_e}, \quad (59b)$$

cf. Prudhomme and Oden (1999) and Ohnibus et al. (2001). Note that the local error norms $\|\mathbf{e}_u|_{\bar{\Omega}_e}\|_{\Omega_e}$ and $\|\mathbf{e}_g|_{\bar{\Omega}_e}\|_{\Omega_e}$ cannot be bounded by an error estimator based on purely local information, since the pollution error cannot be taken into account in this fashion. However, the upper error bound presumably holds due to the Cauchy-Schwarz inequality as the main source of overestimation. As has already been noted, a guaranteed upper bound can only be obtained by the estimate (51) using available energy norm error estimators of equilibrated residual type based on local Neumann problems.

Summarizing the above presented strategies for a posteriori error estimation (57), (58), (59) and (51) it needs to be emphasized that upper error bounds on the error measure $|E(\mathbf{u}, \mathbf{u}_h)|$ can be obtained, but the “more guaranteed” they are, the less sharp they become. We further remark that the presented estimators (59) and (51), which are based on the Cauchy-Schwarz inequality, are restricted to self-adjoint problems, whereas the estimators (57) and (58) are more versatile. Moreover, it should be pointed out that in the case where the goal-quantity of interest Q is defined as in (30), all estimates (52a) - (52d) simplify to the identity $E(\mathbf{u}, \mathbf{u}_h) = a(\mathbf{e}_u, \mathbf{e}_u)$.

In what follows we shall derive two principally different strategies to compute the still abstract a posteriori error estimators (57), (58) and (59). Furthermore, we present a guaranteed upper bound in the sense of the estimate (51).

4.2 Equilibrated Residual Error Estimators based on Local Neumann Problems

In the first strategy, we will apply the well-known approach of solving, in turn, local Neumann problems for the primal as well as for the dual problem to obtain, in a first step, guaranteed upper error bounds for an energy norm control of the errors \mathbf{e}_u and \mathbf{e}_g . This global a posteriori error estimator (for the primal problem) is originally due to Bank and Weiser (1985) and Ainsworth and Oden (1993). The main idea of this residual type error estimator is to solve the variational problems (24) and (43) for the errors \mathbf{e}_u and \mathbf{e}_g , respectively, in a cost effective fashion, i.e. locally on element level.

As a point of departure, let us introduce the “broken” space $\mathcal{V}_{br} = \{\mathbf{v} \in [L_2(\Omega)]^3; \mathbf{v}|_{\bar{\Omega}_e} \in \mathcal{V}_e \ \forall \bar{\Omega}_e\}$ associated with the local test and solution space \mathcal{V}_e . Since $\mathcal{V}_{br} \supseteq \mathcal{V}$, we have to extend the weak forms of the residuals $R_{phy,u}$ and $\bar{R}_{phy,g}$, originally defined on \mathcal{V} , to the broken space \mathcal{V}_{br} . We do so introducing additionally equilibrated tractions $\mathbf{t}_{phy,e} \in [L_2(\partial\Omega_e)]^3$ on the element boundaries $\partial\Omega_e$ for both the primal and the dual problem. Hence, the extended functionals $\tilde{R}_{phy,u} : \mathcal{V}_{br} \rightarrow \mathbb{R}$ and $\tilde{\bar{R}}_{phy,g} : \mathcal{V}_{br} \rightarrow \mathbb{R}$ are given by

$$\tilde{R}_{phy,u}(\mathbf{v}) = \sum_{n_e} \tilde{R}_{phy,u,e}(\mathbf{v}|_{\bar{\Omega}_e}) \quad \forall \mathbf{v} \in \mathcal{V}_{br} \quad (60)$$

and

$$\tilde{\bar{R}}_{phy,g}(\mathbf{v}) = \sum_{n_e} \tilde{\bar{R}}_{phy,g,e}(\mathbf{v}|_{\bar{\Omega}_e}) \quad \forall \mathbf{v} \in \mathcal{V}_{br}, \quad (61)$$

respectively. Here, $\tilde{R}_{phy,u,e} : \mathcal{V}_e \rightarrow \mathbb{R}$ and $\tilde{\bar{R}}_{phy,g,e} : \mathcal{V}_e \rightarrow \mathbb{R}$ are the restrictions of $\tilde{R}_{phy,u}$ and $\tilde{\bar{R}}_{phy,g}$ to an element $\bar{\Omega}_e$ given by

$$\tilde{R}_{phy,u,e}(\mathbf{v}_e) = \int_{\partial\Omega_e} \tilde{\mathbf{t}}_{phy,e} \cdot \mathbf{v}_e \, dS - a_e(\mathbf{u}_h|_{\bar{\Omega}_e}, \mathbf{v}_e) \quad (62)$$

and

$$\tilde{\tilde{R}}_{phy,g,e}(\mathbf{v}_e) = E_{T,e}(\mathbf{v}_e) + \int_{\partial\Omega_e} \tilde{\mathbf{t}}_{phy,e} \cdot \mathbf{v}_e \, dS - a_e^*(\mathbf{g}_h|_{\bar{\Omega}_e}, \mathbf{v}_e), \quad (63)$$

respectively, where $E_{T,e}$ represents the restriction of E_T to an element $\bar{\Omega}_e$. Apparently, it is necessary that the equilibrated tractions $\tilde{\mathbf{t}}_{phy,e}$ are constructed in such a fashion that $\tilde{R}_{phy,u}(\mathbf{v}) = R_{phy,u}(\mathbf{v})$ and $\tilde{\tilde{R}}_{phy,g}(\mathbf{v}) = \bar{R}_{phy,g}(\mathbf{v})$ for all $\mathbf{v} \in \mathcal{V}$. Thus, from the definitions of the extended weak forms $\tilde{R}_{phy,u}$ and $\tilde{\tilde{R}}_{phy,g}$ and the weak forms of the residuals (60) and (61), we recognize that

$$\sum_{n_e} \int_{\partial\Omega_e} \tilde{\mathbf{t}}_{phy,e} \cdot \mathbf{v}|_{\bar{\Omega}_e} \, dS = \int_{\Gamma_N} \bar{\mathbf{t}}_{phy} \cdot \mathbf{v} \, dS \quad \forall \mathbf{v} \in \mathcal{V}. \quad (64)$$

This condition can easily be fulfilled if the equilibrated tractions $\tilde{\mathbf{t}}_{phy,e}$ coincide with the Neumann boundary conditions $\tilde{\mathbf{t}}_{phy,e} = \bar{\mathbf{t}}_{phy}$ on $\partial\Omega_e \cap \Gamma_N$ and fulfill the lemma of Cauchy $\tilde{\mathbf{t}}_{phy,e} = -\bar{\mathbf{t}}_{phy,f}$ on $\bar{\Omega}_e \cap \bar{\Omega}_f$. Note carefully that the right hand side of (64) vanishes in case of the dual problem.

Recalling the error representation formula (24), we are now in the position to introduce the corresponding local problem, which is a pure Neumann problem, as follows: find a solution $\varphi_e \in \mathcal{V}_e$ that satisfies

$$a_e(\varphi_e, \mathbf{v}_e) = \tilde{R}_{phy,u,e}(\mathbf{v}_e) \quad \forall \mathbf{v}_e \in \mathcal{V}_e. \quad (65)$$

Similarly, in case of the dual problem we solve the associated local problem

$$a_e^*(\chi_e, \mathbf{v}_e) = \tilde{\tilde{R}}_{phy,g,e}(\mathbf{v}_e) \quad \forall \mathbf{v}_e \in \mathcal{V}_e \quad (66)$$

for $\chi_e \in \mathcal{V}_e$. For the well-posedness of these local problems the bilinear forms a_e and a_e^* are assumed to be $\mathcal{V}_e/\mathcal{L}_e$ - and $\mathcal{V}_e/\mathcal{L}_e^*$ -elliptic, respectively, where $\mathcal{L}_e = \{\mathbf{w}_e \in \mathcal{V}_e; a_e(\mathbf{w}_e, \mathbf{v}_e) = 0 \, \forall \mathbf{v}_e \in \mathcal{V}_e\}$ and $\mathcal{L}_e^* = \{\mathbf{w}_e \in \mathcal{V}_e; a_e^*(\mathbf{w}_e, \mathbf{v}_e) = 0 \, \forall \mathbf{v}_e \in \mathcal{V}_e\}$ denote the spaces of rigid body motions, i.e. the kernels of the bilinear forms a_e and a_e^* . In other words, the rigid body motions have to be filtered out for the solvability of (65) and (66). Moreover, the equilibrated tractions $\tilde{\mathbf{t}}_{phy,e}$ have to be in equilibrium with the interior loads obtained from the finite element solutions $\mathbf{u}_h \in \mathcal{V}_h$ and $\mathbf{g}_h \in \mathcal{V}_h$. Thus, the equilibration conditions

$$\tilde{R}_{phy,u,e}(\mathbf{v}_e) = 0 \quad \forall \mathbf{v}_e \in \mathcal{L}_e \quad \text{and} \quad \tilde{\tilde{R}}_{phy,g,e}(\mathbf{v}_e) = 0 \quad \forall \mathbf{v}_e \in \mathcal{L}_e^* \quad (67)$$

must be fulfilled in either case, which leads to conditional equations for the determination of the (nonunique) equilibrated tractions $\tilde{\mathbf{t}}_{phy,e}$. Here, we will closely follow the approach originally proposed by Ladevèze and Leguillon (1983) to compute the equilibrated tractions $\tilde{\mathbf{t}}_{phy,e}$, see also Brink and Stein (1998). The basic idea of improving the approximate tractions can be traced back to Buefler and Stein (1970) and Stein and Ahmad (1977).

Once the equilibrated tractions $\tilde{\mathbf{t}}_{phy,e}$ are determined and the Neumann problems (65) and (66) are solved, all that remains is to show how an upper error bound can be computed. To this end, let us recall that the equilibrated tractions $\tilde{\mathbf{t}}_{phy,e}$ were constructed such that $\sum_{n_e} \tilde{R}_{phy,u,e}(\mathbf{v}|_{\bar{\Omega}_e}) = R_{phy,u}(\mathbf{v})$ and $\sum_{n_e} \tilde{\tilde{R}}_{phy,g,e}(\mathbf{v}|_{\bar{\Omega}_e}) = \bar{R}_{phy,g}(\mathbf{v})$ hold, which is expressed in (64). With the error representation formulas (24) and (43) we have thus found that

$$a(\mathbf{e}_u, \mathbf{v}) = \sum_{n_e} a_e(\varphi_e, \mathbf{v}|_{\bar{\Omega}_e}) \quad \forall \mathbf{v} \in \mathcal{V} \quad (68)$$

and, in case of the dual problem,

$$a^*(\mathbf{e}_g, \mathbf{v}) = \sum_{n_e} a_e^*(\chi_e, \mathbf{v}|_{\bar{\Omega}_e}) \quad \forall \mathbf{v} \in \mathcal{V}. \quad (69)$$

Following Ainsworth and Oden (2000), it can be shown that upon applying the Cauchy-Schwarz inequality twice on (68) and (69) we are led to the (global) a posteriori error estimators

$$\|\mathbf{e}_u\| \leq \left\{ \sum_{n_e} \|\varphi_e\|_{\bar{\Omega}_e}^2 \right\}^{\frac{1}{2}} \quad (70)$$

and

$$\|\mathbf{e}_g\| \leq \left\{ \sum_{n_e} \|\chi_e\|_{\bar{\Omega}_e}^2 \right\}^{\frac{1}{2}} \quad (71)$$

without any multiplicative constants. It needs to be emphasized, however, that these bounds are only guaranteed for functions belonging to the infinite dimensional space \mathcal{V}_e . Hence, in a finite element code higher order ansatz functions are implemented to retain the upper bound property of the estimator.

As mentioned earlier, upon inserting the above energy norm error estimators (70) and (71) into (51) we thus arrive at the following a posteriori error estimator with guaranteed upper bounds

$$|E(\mathbf{u}, \mathbf{u}_h)| \leq \left\{ \sum_{n_e} \|\varphi_e\|_{\Omega_e}^2 \right\}^{\frac{1}{2}} \left\{ \sum_{n_e} \|\chi_e\|_{\Omega_e}^2 \right\}^{\frac{1}{2}}. \quad (72)$$

Now, let us recall the local Neumann problems (65) and (66). Since these problems are local forms of the exact error representations (24) and (48) one might consider their solutions $\varphi_e \in \mathcal{V}_e$ and $\chi_e \in \mathcal{V}_e$ as approximations of the error contributions $\mathbf{e}_u|_{\bar{\Omega}_e} \in \mathcal{V}_e$ and $\mathbf{e}_g|_{\bar{\Omega}_e} \in \mathcal{V}_e$, respectively – in the sense of (54) – up to possible rigid body motions. Indeed, if the equilibrated tractions $\mathbf{t}_{phy,e}$ are the exact tractions $\mathbf{t}_{phy}(\mathbf{u}|_{\bar{\Omega}_e})$, for the primal problem, and $\mathbf{t}_{phy}(\mathbf{g}|_{\bar{\Omega}_e})$ in case of the dual problem, then we easily obtain $\varphi_e = \mathbf{e}_u|_{\bar{\Omega}_e}$ and $\chi_e = \mathbf{e}_g|_{\bar{\Omega}_e}$. It is quite evident that in this special case the broken space \mathcal{V}_{br} equals the test and solution space \mathcal{V} , since no jumps occur on the interelement boundaries. With the solutions φ_e and χ_e at hand we may now compute the presented a posteriori error estimators (57), (58) and (59). Recalling the general strategy (52) and summarizing the presented error estimators of equilibrated residual type reveals that

$$\sum_{n_e} a_e(\varphi_e, \chi_e) \leq \sum_{n_e} |a_e(\varphi_e, \chi_e)| \leq \sum_{n_e} \|\varphi_e\|_{\Omega_e} \|\chi_e\|_{\Omega_e} \leq \left\{ \sum_{n_e} \|\varphi_e\|_{\Omega_e}^2 \right\}^{\frac{1}{2}} \left\{ \sum_{n_e} \|\chi_e\|_{\Omega_e}^2 \right\}^{\frac{1}{2}}. \quad (73)$$

It should be carefully noted, however, that this order – contrarily to the estimate (52) – is not guaranteed. For the sake of clearness, in view of the numerical example in Section 5 the error estimators (73) are henceforth denoted as “residual 1”, “residual 2”, “residual 3” and “residual 4” (from left to right).

4.3 Averaging Techniques

Another widely used technique to control the finite element discretization error in the energy norm was originally proposed by Zienkiewicz and Zhu (1987) and is based on averaging techniques or, more precisely, on recovery of the approximate stress field $\sigma(\mathbf{u}_h)$. Recently, Carstensen and Funken (2001) have shown the reliability of averaging estimators, if all geometrical and physical data are smooth enough. Therefore, we shall discuss below in greater detail how a recovery technique can be applied to estimate the error measure E .

To begin with, we recall the error estimators (57), (58) and (59) (which are henceforth denoted as “averaging 1”, “averaging 2” and “averaging 3”, respectively) as presented in the preceding section. It is readily seen that the secret of an efficient estimator is the local, i.e. element- or patchwise approximation of error contributions. Following Zienkiewicz and Zhu (1987), this can be established by introducing the complementary energy and subsequent recovery of the stresses. Hence, we may introduce the approximation

$$a_e(\mathbf{e}_u|_{\bar{\Omega}_e}, \mathbf{e}_g|_{\bar{\Omega}_e}) \approx a_e(\varphi_e, \chi_e) = \int_{\Omega_e} \sigma(\varphi_e) : \mathbb{C}^{-1} : \sigma(\chi_e) \, dV \quad (74)$$

as used in the error estimators (57) and (58) as well as

$$\|\mathbf{e}_u|_{\bar{\Omega}_e}\|_{\Omega_e}^2 \approx a_e(\varphi_e, \varphi_e) = \int_{\Omega_e} \sigma(\varphi_e) : \mathbb{C}^{-1} : \sigma(\varphi_e) \, dV \quad (75a)$$

$$\|\mathbf{e}_g|_{\bar{\Omega}_e}\|_{\Omega_e}^2 \approx a_e(\chi_e, \chi_e) = \int_{\Omega_e} \sigma(\chi_e) : \mathbb{C}^{-1} : \sigma(\chi_e) \, dV \quad (75b)$$

in case of the estimator (59), where \mathbb{C}^{-1} denotes the fourth-order tensor of elastic compliances. By the linearity of the stress tensor σ we get

$$\sigma(\varphi_e) = \sigma^*(\mathbf{u}_h|_{\bar{\Omega}_e}) - \sigma(\mathbf{u}_h|_{\bar{\Omega}_e}) \quad (76a)$$

$$\sigma(\chi_e) = \sigma^*(\mathbf{g}_h|_{\bar{\Omega}_e}) - \sigma(\mathbf{g}_h|_{\bar{\Omega}_e}), \quad (76b)$$

where $\sigma^*(\mathbf{u}_h|_{\bar{\Omega}_e})$ and $\sigma^*(\mathbf{g}_h|_{\bar{\Omega}_e})$ are recovered stress fields from the finite element solutions $\mathbf{u}_h \in \mathcal{V}_h$ and $\mathbf{g}_h \in \mathcal{V}_h$, respectively.

What remains to show is how the recovered stress fields $\sigma^*(\mathbf{u}_h)$ and $\sigma^*(\mathbf{g}_h)$ can be computed. For the sake of conciseness, we shall restrict our considerations to the case of recovering $\sigma^*(\mathbf{u}_h)$, since the general procedure is the same for both considered stress fields. Basically, the approximated stress field $\sigma(\mathbf{u}_h)$ involves gradients of the finite element solution $\mathbf{u}_h \in \mathcal{V}_h$. Hence, by definition of the space $\mathcal{V}_h \subset \mathcal{V}$, it is easy to see that the approximated stress field is generally discontinuous on the interelement boundaries and therefore contradicts with the exact (in most cases) smooth solution. Thus, it is obvious to assume that a smoothed stress field $\sigma^*(\mathbf{u}_h)$ might lead to a better approximation of stresses (in most cases), which can easily be achieved by taking the same ansatz functions for the stresses as for the C^0 -continuous displacement field. As a consequence, appropriate nodal values $\hat{\sigma}^*$ of the stresses are required. For this purpose, different strategies were developed in recent years. One of those is the so-called Superconvergent Patch Recovery (SPR) technique, introduced by Zienkiewicz and Zhu (1992), which we apply here.

5 Numerical Example

The purpose of the present section is to present an illustrative numerical example that shows the performance of the a posteriori error estimators as derived in the preceding section.

In this paper we restrict our considerations to the linear elasticity theory and therefore to materials well-known for their brittle material behavior. More precisely, we make the choice of the inorganic and amorphous material glass at room temperature, since the use of glass – as one of the oldest building materials – in structural engineering has enormously increased in recent years. The (theoretical) strength of glass products is rather high. However, from a practical point of view the strength is considerably reduced by a huge amount of surface flaws in the range from microcracks, introduced during manufacture, up to large macroscopic cracks caused by material damage. Therefore, investigations on the fracture behavior of glass within the framework of linear elasticity theory and linear elastic fracture mechanics are of the utmost importance.

5.1 Single Edge Cracked Tension (SECT) Specimen

In the numerical example let us consider a single edge cracked tension (SECT) specimen made of glass in plane stress state. Obviously, by symmetry considerations, only one half of the SECT specimen needs to be modeled, as depicted in Figure 1. In this example, the finite element subspace \mathcal{V}_h is constructed by using bilinear isoparametric Q_1 -elements. For the chosen material glass, the following material data are assumed: Young's modulus $E = 70000 \text{ N/mm}^2$ and Poisson's ratio $\nu = 0,29$. Furthermore, the (primal) load on top of the specimen is chosen as $F = 0,7 \text{ N/mm}^2$.

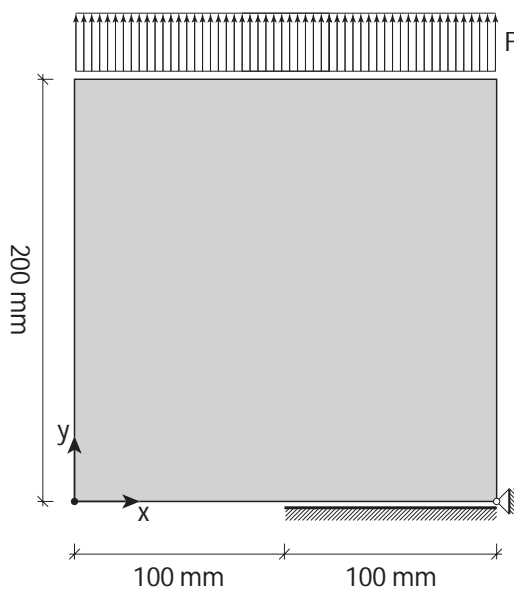


Figure 1: Modeled single edge cracked tension specimen, primal loading and measurements.

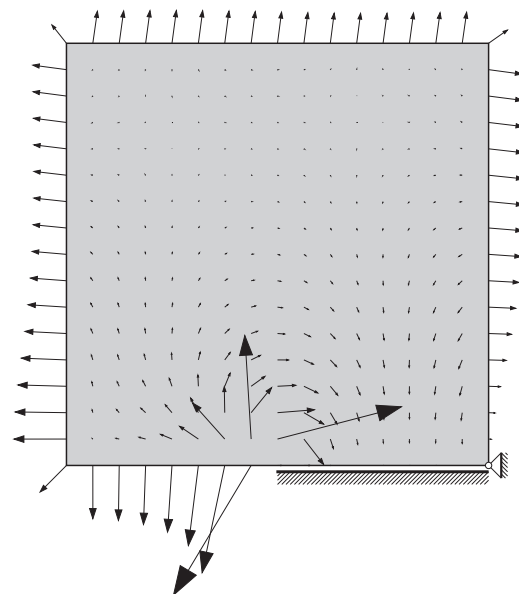


Figure 2: Modeled single edge cracked tension specimen and dual loading.

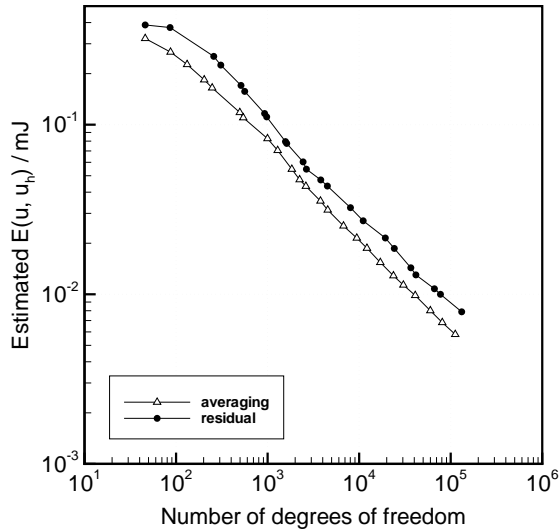


Figure 3: Newtonian mechanics: Estimated errors.

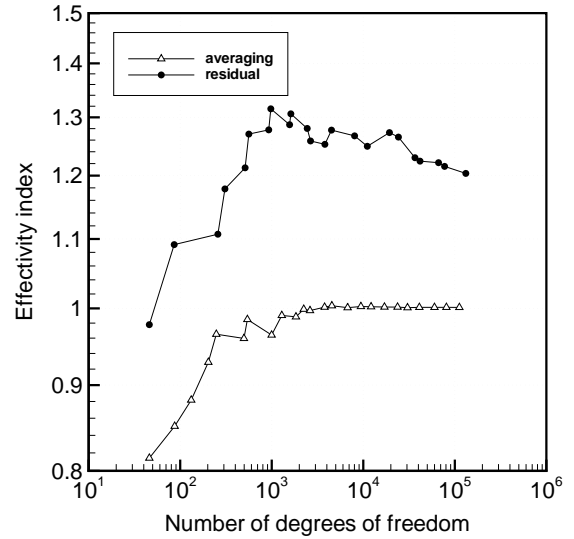


Figure 4: Newtonian mechanics: Effectivity indices.

In a first computation we aim at controlling the error e_u measured by the energy norm within Newtonian mechanics. The applied adaptive mesh refinement strategy for all computations in this paper reads as follows: an element is refined, if the scaled error indicator, i.e. the estimated error divided by the maximum estimated error on element level, is larger than a predefined tolerance $\theta \in (0, 1)$ which was set here to $\theta = 0,5$. The convergence of the estimated error, as obtained by the equilibrated residual error estimator based on local Neumann problems and by the averaging technique based on the SPR technique can be seen in Figure 3. Here, it can be observed that both error estimators yield an optimal convergence rate.

The associated effectivity indices, i.e. the ratios of the estimated errors to the true error, are plotted in Figure 4. A reference solution for the exact value $\|\mathbf{u}\|$ was obtained on an adaptively refined mesh based on biquadratic isoparametric Q_2 -elements with 132740 degrees of freedom (dof) and became $\|\mathbf{u}\| \approx \|\mathbf{u}_h\| = 0.84116936$ mJ. The effectivity indices show that the residual error estimator yields, as expected, a guaranteed upper bound on the error measure E , which is also quite sharp. Only for the coarse start mesh we do not observe an upper error bound. This is simply because the local Neumann problems are solved with only one order higher ansatz functions, i.e. $p = 2$. With increasing polynomial order p the upper bound can also be retained on a coarse mesh. An astonishingly sharp estimate of the error (around the desired value “1”) can be obtained by using the averaging technique. With the latter error estimator, however, we do not obtain an upper bound on the error measure E as can be verified by means of Figure 4.

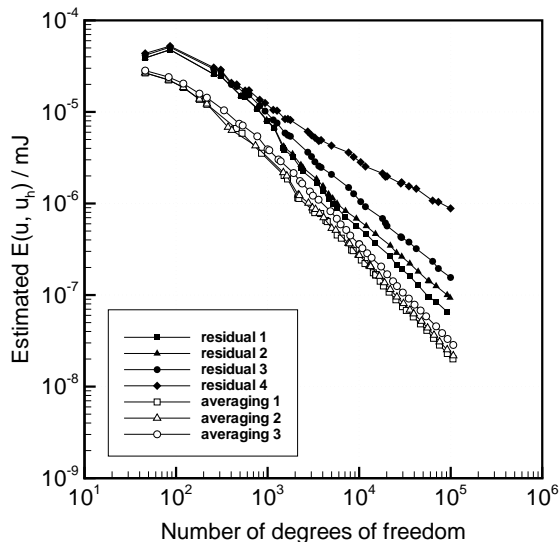


Figure 5: Eshelbian mechanics: Estimated errors.

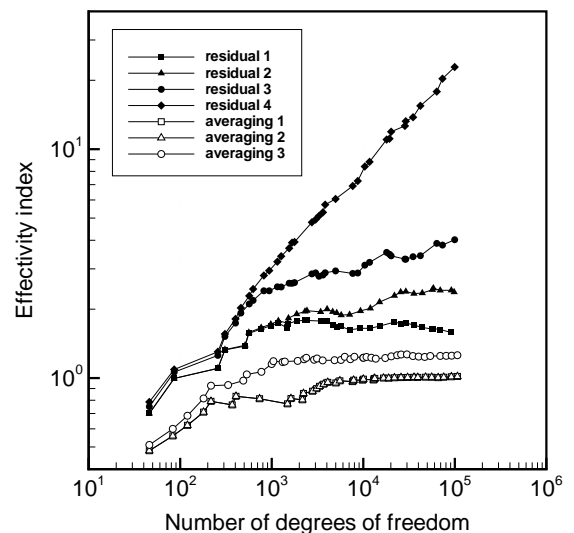


Figure 6: Eshelbian mechanics: Effectivity indices.

In a second computation, let us investigate how the finite element discretization error e_u can be controlled within Eshelbian mechanics by means of the global functional (31). Therefore, we first have to solve the associated dual problem. The dual load is depicted in Figure 2. Here it can be seen that high loads occur on the Neumann boundary Γ_N and in the region around the crack tip with (Cauchy) stress singularity of $r^{-\frac{1}{2}}$ -type. Moreover, the “global” character of the Eshelby functional $b(\mathbf{u}, \mathbf{u})$ can be verified, since loads appear in the entire domain Ω .

As can be seen from Figure 5, the convergence of the error estimators is much higher now compared to the energy norm error estimator of the previous computation. This is simply due to the fact that the energy norm is the square root of the functional $a(\mathbf{u}, \mathbf{u})$, whereas in Eshelbian mechanics we consider the functional $b(\mathbf{u}, \mathbf{u})$. Furthermore, it can be observed that the guaranteed upper bound error estimator “residual 4” does not yield an optimal convergence rate, whereas the remaining error estimators show a good convergence. Remarkably, all error estimators of averaging type are rather close to each other and yield lower values for the estimated error measure than the residual type error estimators.

Virtually the same results can be observed by means of the associated effectivity indices as plotted in Figure 6. Again, the averaging type error estimators yield rather sharp error estimates around “1”. Note, however, that no error bounds can be obtained in this fashion. The residual error estimators show bounds on the error measure E , but they are not as sharp as the averaging error estimators. We remark that in this numerical example all residual error estimators yield an upper error bound (except for the coarse start mesh), although from the theory only the upper bound as obtained from “residual 4” is guaranteed. However, this upper bound is comparatively high due to the before mentioned overestimation resulting from the Cauchy-Schwarz inequality, since the angle between the errors e_u and e_g can become rather large.

Next, let us compare the finite element meshes as obtained in Newtonian and in Eshelbian mechanics. As can be verified from Figures 7 and 8, where the mesh is plotted on the magnified deformed structure, both meshes look rather similar for about the same number of degrees of freedom. Clearly, heavy mesh refinement takes place at the crack tip because of the stress singularity at this point.

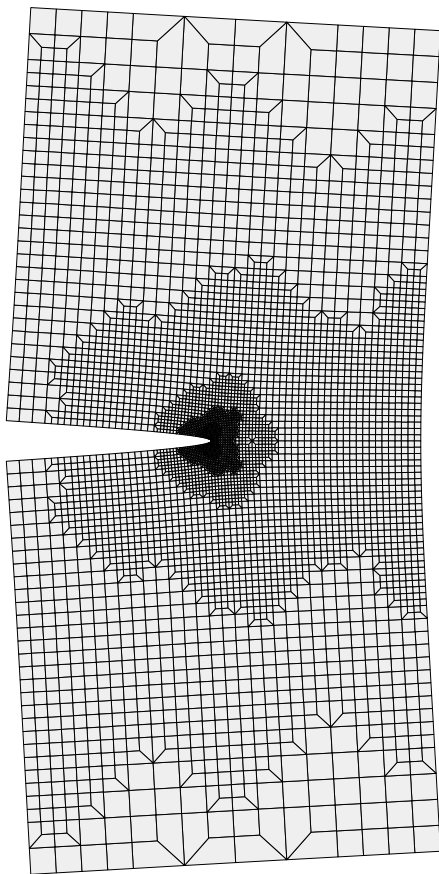


Figure 7: Newtonian mechanics: primal solution, 15th adaptively refined mesh, 6743 dof (for the modeled system), “averaging” estimator, deformed structure (displacements are magnified a 1000 times).

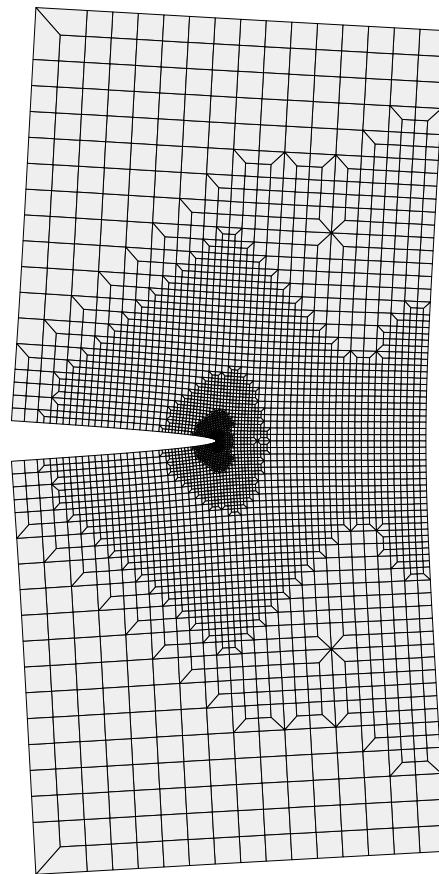


Figure 8: Eshelbian mechanics: primal solution, 19th adaptively refined mesh, 6389 dof (for the modeled system), “averaging 1” estimator, deformed structure (displacements are magnified a 1000 times).

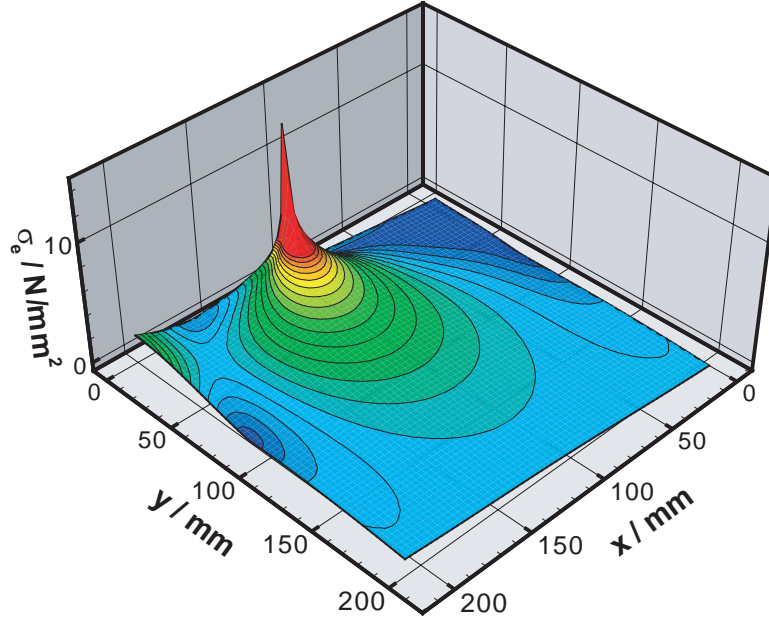


Figure 9: Newtonian mechanics: Equivalent Cauchy stress σ_e , deformed configuration (displacements are magnified a 1000 times).

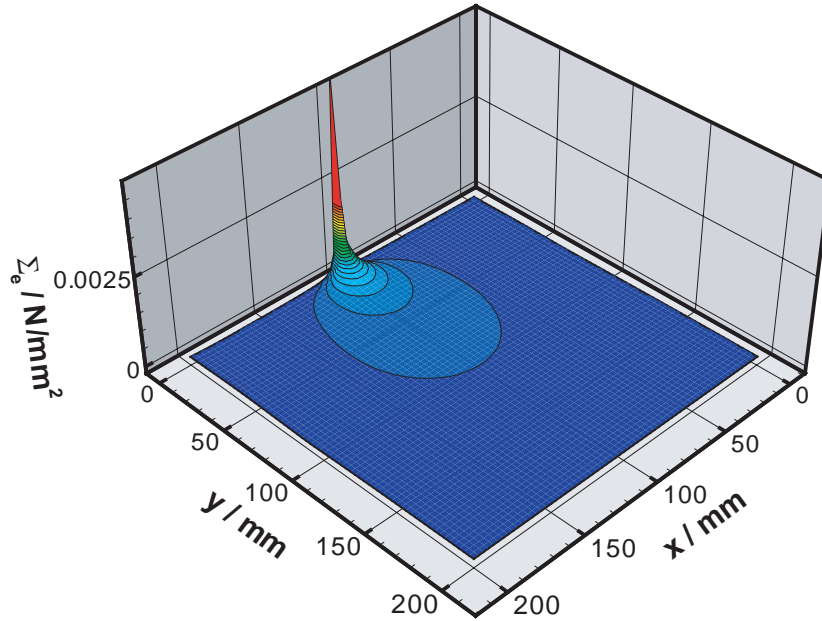


Figure 10: Eshelbian mechanics: Equivalent Newton-Eshelby stress Σ_e , undeformed configuration.

The stress singularity (of the Cauchy stress) can also be verified by means of the distribution of the equivalent Cauchy stress $\sigma_e = \sqrt{3/2} \operatorname{dev} \boldsymbol{\sigma} : \operatorname{dev} \boldsymbol{\sigma}$ as depicted in Figure 9. Clearly, within the framework of Eshelbian mechanics we also obtain a stress singularity in the Newton-Eshelby stress. In this case we observe a singularity of r^{-1} -type. Similarly to Figure 9 the stress singularity is visualized in Figure 10 where analogously to the equivalent Cauchy stress σ_e the equivalent Newton-Eshelby stress, defined as $\Sigma_e = \sqrt{3/2} \operatorname{dev} \boldsymbol{\Sigma} : \operatorname{dev} \boldsymbol{\Sigma}$, is plotted. Note that apart from the vicinity of the crack tip, the equivalent Newton-Eshelby stress is vanishingly small in the remaining part of the domain Ω .

Finally, let us consider the distribution of discrete material forces within the framework of Eshelbian mechanics on different meshes. In other words, we consider the distribution of discrete material forces as obtained by different finite element solutions $\mathbf{u}_{h,1}$ and $\mathbf{u}_{h,2}$ in different finite element subspaces $\mathcal{V}_{h,1}$ and $\mathcal{V}_{h,2}$, respectively, whereby $\mathcal{V}_{h,1} \subset \mathcal{V}_{h,2}$, since $\mathcal{V}_{h,2}$ is constructed by using more elements. Since the mesh is adapted with respect to the chosen error measure $E(\mathbf{u}, \mathbf{u}_h) = b(\mathbf{u}, \mathbf{u}) - b(\mathbf{u}_h, \mathbf{u}_h)$, the finite element solution $\mathbf{u}_{h,2}$ is better than $\mathbf{u}_{h,1}$ and

therefore closer to the exact solution \mathbf{u} in the sense that $|E(\mathbf{u}, \mathbf{u}_{h,2})| < |E(\mathbf{u}, \mathbf{u}_{h,1})|$. Hence, one can expect that the residual material forces become smaller on the finer mesh which can be verified by means of Figures 11 and 12. Since the material is homogeneous, for the exact solution \mathbf{u} no material forces occur in the domain Ω . However, at the crack tip a material force arises in the opposite direction of crack propagation. The length of this material force equals the value of the well-known J -integral and can therefore be used as a fracture criterion in linear elastic fracture mechanics. Now, let us consider the coarse start mesh as plotted in Figure 11. Here, we observe residual material forces e.g. at the points P_1 and P_2 with coordinates $(100, 50)$ and $(50, 0)$, respectively. Figure 12 shows that these residual material forces nearly vanish during adaptive mesh refinements. However, new residual material forces arise closer to the crack tip. Clearly, these residual material forces will also (nearly) vanish with increasing adaptive mesh refinements.

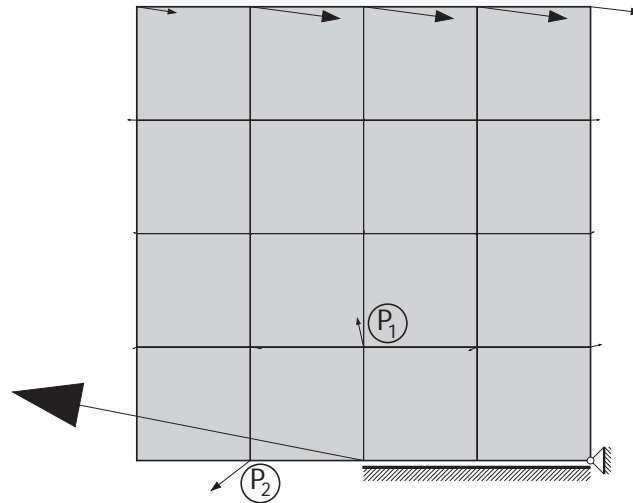


Figure 11: Distribution of discrete material forces, coarse mesh (start mesh), 46 dof.

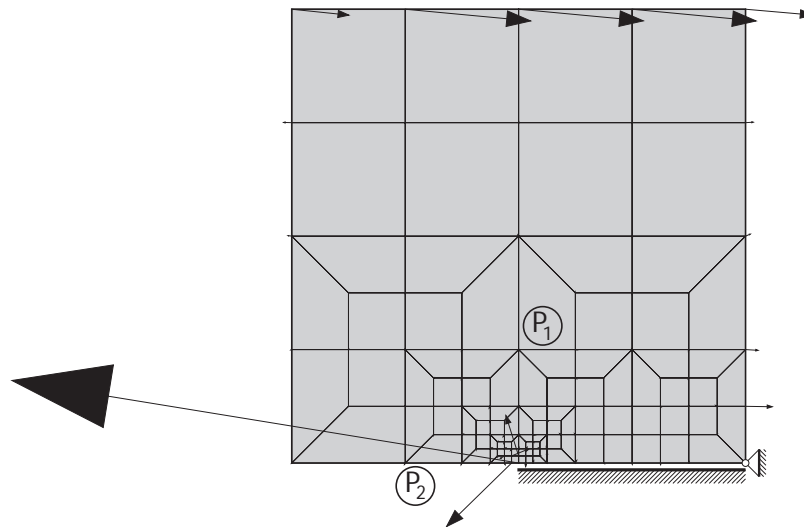


Figure 12: Distribution of discrete material forces, 5th adaptively refined mesh, 217 dof.

6 Conclusions

In this paper we presented residual and averaging type global a posteriori error estimators within the frameworks of Newtonian and Eshelbian mechanics. Upon introducing the exact error representation formulas for the finite element discretization error, the error estimators were derived in Newtonian mechanics by equilibrating the tractions on the interelement boundaries or by recovery of the stress fields. In order to derive error estimators in Eshelbian mechanics, an auxiliary dual problem in the Newtonian setting had to be solved, since the Galerkin orthogonality does not hold in Eshelbian mechanics. Finally, in a numerical example we obtained good numerical evidence for both the upper bound property of the residual error estimator and the sharpness of the averaging technique.

References

- Ainsworth, M.; Oden, J.: A unified approach to a posteriori error estimation based on element residual methods. *Numer. Math.*, 65, (1993), 23–50.
- Ainsworth, M.; Oden, J.: *A posteriori error estimation in finite element analysis*. John Wiley & Sons, New York (2000).
- Babuška, I.; Strouboulis, T.: *The Finite Element Method and its Reliability*. Oxford University Press, Oxford (2001).
- Bank, R.; Weiser, A.: Some a posteriori error estimators for elliptic partial differential equations. *Math. Comp.*, 44, (1985), 283–301.
- Becker, R.; Rannacher, R.: A feed-back approach to error control in finite element methods: Basic analysis and examples. *East-West J. Numer. Math.*, 4, (1996), 237–264.
- Brink, U.; Stein, E.: A posteriori error estimation in large-strain elasticity using equilibrated local Neumann problems. *Comput. Methods Appl. Mech. Engrg.*, 161, (1998), 77–101.
- Bufler, H.; Stein, E.: Zur Plattenberechnung mittels Finiter Elemente. *Ing. Archiv*, 39, (1970), 248–260.
- Carstensen, C.; Funken, S.: Averaging technique for FE - a posteriori error control in elasticity. Part I: Conforming FEM. *Comput. Methods Appl. Mech. Engrg.*, 190, (2001), 2483–2498.
- Cirak, F.; Ramm, E.: A posteriori error estimation and adaptivity for linear elasticity using the reciprocal theorem. *Comput. Methods Appl. Mech. Engrg.*, 156, (1998), 351–362.
- Eriksson, K.; Estep, D.; Hansbo, P.; Johnson, C.: Introduction to adaptive methods for differential equations. *Acta Numer.*, pages 106–158.
- Eshelby, J.: The force on an elastic singularity. *Philos. Trans. Roy. Soc. London Ser. A*, 244, (1951), 87–112.
- Heintz, P.; Larsson, F.; Hansbo, P.; Runesson, K.: On error control and adaptivity for computing material forces in fracture mechanics. In: H. Mang; F. Rammerstorfer; J. Eberhardsteiner, eds., *WCCM V – Fifth World Congress on Computational Mechanics, Vienna, Austria* (2002).
- Kienzler, R.; Herrmann, G.: *Mechanics in Material Space – with Applications to Defect and Fracture Mechanics*. Springer-Verlag, Berlin (2000).
- Kuhl, E.; Askes, H.; Steinmann, P.: An energy minimizing mesh optimisation strategy based on the equilibration of discrete spatial and material forces. In: N.-E. Wiberg; P. Díez, eds., *ADMOS – International Conference on Adaptive Modeling and Simulation, Göteborg, Sweden* (2003).
- Ladevèze, P.; Leguillon, D.: Error estimate procedure in the finite element method and applications. *SIAM J. Numer. Anal.*, 20, (1983), 485–509.
- Larsson, F.; Hansbo, P.; Runesson, K.: On the computation of goal-oriented a posteriori error measures in nonlinear elasticity. *Int. J. Numer. Methods Engrg.*, 55, (2002), 879–894.
- Maugin, G.: *Material Inhomogeneities in Elasticity*. Chapman & Hall, London (1993).
- Mueller, R.; Maugin, G.: On material forces and finite element discretizations. *Comp. Mech.*, 29, (2002), 52–60.
- Ohnibus, S.; Stein, E.; Walhorn, E.: Local error estimates of FEM for displacements and stresses in linear elasticity by solving local Neumann problems. *Int. J. Numer. Methods Engrg.*, 52, (2001), 727–746.
- Prudhomme, S.; Oden, J.: On goal-oriented error estimation for local elliptic problems: application to the control of pointwise errors. *Comput. Methods Appl. Mech. Engrg.*, 176, (1999), 313–331.
- Rüter, M.; Stein, E.: Goal-oriented a posteriori error estimates in elastic fracture mechanics. In: H. Mang; F. Rammerstorfer; J. Eberhardsteiner, eds., *WCCM V – Fifth World Congress on Computational Mechanics, Vienna, Austria* (2002).
- Stein, E.; Ahmad, R.: An equilibrium method for stress calculation using finite element methods in solid- and structural-mechanics. *Comput. Methods Appl. Mech. Engrg.*, 10, (1977), 175–198.

- Stein, E.; Rüter, M.; Ohnimus, S.: Adaptive finite element analysis and modeling of solids and structures – findings, problems and trends. *Int. J. Numer. Methods Engrg.*, (2004), in print.
- Steinmann, P.: Application of material forces to hyperelastostatic fracture mechanics. I. Continuum mechanical setting. *Int. J. Solids Structures*, 37, (2000), 7371–7391.
- Steinmann, P.; Ackermann, D.; Barth, F.: Application of material forces to hyperelastostatic fracture mechanics. II. Computational setting. *Int. J. Solids Structures*, 38, (2001), 5509–5526.
- Verfürth, R.: A review of a posteriori error estimation techniques for elasticity problems. *Comput. Methods Appl. Mech. Engrg.*, 176, (1999), 419–440.
- Zienkiewicz, O.; Zhu, J.: A simple error estimator and adaptive procedure for practical engineering analysis. *Int. J. Numer. Methods Engrg.*, 24, (1987), 337–357.
- Zienkiewicz, O.; Zhu, J.: The superconvergent patch recovery and a posteriori error estimates. Part 1: The recovery technique. *Int. J. Numer. Methods Engrg.*, 33, (1992), 1331–1364.

Address: Dr.-Ing. Marcus Rüter and Prof. Dr.-Ing. Dr. E.h. Dr. h.c. mult. Erwin Stein, Institut für Baumechanik und Numerische Mechanik, Universität Hannover, Appelstraße 9A, D-30167 Hannover.
email: rueter@ibnm.uni-hannover.de; stein@ibnm.uni-hannover.de.